

Data release from critical mineral studies of the Kitsault, Huckleberry, and Berg porphyry deposits

Audrey C. Graham, Evan A. Orovan, Corey Wall, Dylan Goudie, Robert Creaser, Daniel Layton-Matthews, and Luke Ootes



Ministry of Mining and Critical Minerals Mine Competitiveness and Authorizations Division British Columbia Geological Survey

Recommended citation: Graham, A.C., Orovan, E., Wall, C., Goudie, D., Creaser, R., Layton-Matthews, D., and Ootes, L., 2025. Data release from critical mineral studies of the Kitsault, Huckleberry, and Berg porphyry deposits. British Columbia Ministry of Mining and Critical Minerals, British Columbia Geological Survey GeoFile 2025-23, 7p

Front cover:

Thin section and corresponding SEM-MLA images showing pyrite-chalcopyrite vein with blebby magnetite and quartz-anhydrite +/- chalcopyrite veinlets cutting silica-sericite-altered Hazelton Group andesite, Huckleberry deposit.

Back cover:

Zircon grains for CA-TIMS geochronology.





Data release from critical mineral studies of the Kitsault, Huckleberry, and Berg porphyry deposits

Audrey C. Graham
Evan A. Orovan
Corey Wall
Dylan Goudie
Robert Creaser
Daniel Layton-Matthews
Luke Ootes

Ministry of Mining and Critical Minerals British Columbia Geological Survey GeoFile 2025-23

Data release from critical mineral studies of the Kitsault, Huckleberry, and Berg porphyry deposits



Audrey C. Graham^{1,a}, Evan A. Orovan¹, Corey Wall², Dylan Goudie³, Robert Creaser⁴, Daniel Layton-Matthews⁵, and Luke Ootes¹

- ¹ British Columbia Geological Survey, Ministry of Mining and Critical Minerals, Victoria, BC, V8W 9N3
- ² Pacific Center for Isotopic and Geochemical Research, Department of Earth, Ocean and Atmospheric Sciences, The University of British Columbia, Vancouver, BC, V6T 1Z4
- ³ Core Research Equipment and Instrument Training (CREAIT) Network, Memorial University of Newfoundland, St. John's, NL, A1C 5S7
- ⁴ Department of Earth and Atmospheric Sciences, University of Alberta, Edmonton, AB, T6G 2R3
- ⁵ Queen's Facility for Isotope Research, Department of Geological Sciences and Geological Engineering, Queen's University, Kingston, ON, K7L 3N6
- ^a Corresponding author: <u>audrey.graham@gov.bc.ca</u>

Recommended citation: Graham, A.C., Orovan, E., Wall, C., Goudie, D., Creaser, R., Layton-Matthews, D., and Ootes, L., 2025. Data release from critical mineral studies of the Kitsault, Huckleberry, and Berg porphyry deposits. British Columbia Ministry of Mining and Critical Minerals, British Columbia Geological Survey GeoFile 2025-23, 7p.

Abstract

Porphyry deposits with primary commodities $Cu \pm Mo \pm Ag \pm Au$ commonly contain concentrations of companion metals (e.g., Te, Bi, Co, Sb, Sn, W). These companion metals, which could conceivably be recovered as by-products, are on the critical mineral lists of many political jurisdictions. Although post-accretionary Cretaceous and Eocene porphyry deposits in British Columbia have been extensively studied and developed, the amount and distribution of companion metals in these deposits remains unclear. The bulk-rock geochemical data for 100 mineralized drill core and rock samples, and geochronologic data from the Kitsault, Huckleberry, and Berg, deposits presented herein will help address uncertainties. Geochronologic data include: 1) LA-ICP-MS U-Pb and trace element geochemical igneous zircon data from Kitsault (n=2), Huckleberry (n=2), and Berg (n=3); 2) high-precision CA-TIMS igneous zircon data from the same samples; and 3) Re-Os geochronology data from molybdenite at Kitsault (n=2), Huckleberry (n=2), and the nearby Whiting Creek project (n=2). Data are also included from sulfur isotope analysis on samples from Kitsault (n=32), Huckleberry (n=60), and Berg (n=32). Scanning electron microprobe-mineral liberation analysis (SEM-MLA) images of thin sections from Kitsault (n=8), Huckleberry (n=12), and Berg (n=9) are presented with accompanying geochemical data.

Keywords: Post-accretionary, porphyry, transitional veins, critical minerals, companion metals

1. Introduction

Primary commodities Cu, Au, Ag, and Mo have long-been produced from porphyry deposits in the Stikine, Quesnel, and Wrangell terranes of the British Columbian Cordillera (Fig. 1). Porphyry deposits are commonly classified as alkalic (Cu-Au) or calc-alkalic and formed: 1) in the late Triassic to early Jurassic before terrane accretion to North America; and 2) in the Cretaceous to Eocene in continental settings following accretion of the allochthonous terranes to North America. All varieties of porphyry deposits may also contain 'companion metals' (John and Taylor, 2016; Mudd et al., 2014, 2017; Nassar et al., 2015) that are on the critical minerals lists of different political jurisdictions (e.g., Hickin et al., 2024), including the 2024 iteration of the Canadian list (NRCan, 2024). These critical companion metals (e.g., Te, Bi, PGM)

could conceivably be recovered as by-products of primary commodity mining (e.g., IGF, 2023).

Studies of critical companion metals in porphyry and related skarn and epithermal deposits in the province have been limited (e.g., Lawley et al., 2025) and thus their distributions remain largely unknown. Herein (BCGS_GF2025-23.zip) we present geochemical, geochronologic, sulphur isotope, and scanning electron microprobe-mineral liberation analysis (SEM-MLA) data from three post-accretionary Cu-Mo porphyries: the past-producing Kitsault and Huckleberry mines and the Berg deposit (Fig. 1). Included are: geochemistry sample metadata and results including quality assurance (Appendix 1); geochronology sample metadata with coordinates, descriptions, and interpreted age summaries (Appendix 2); data from laser ablation inductively coupled plasma mass spectrometry

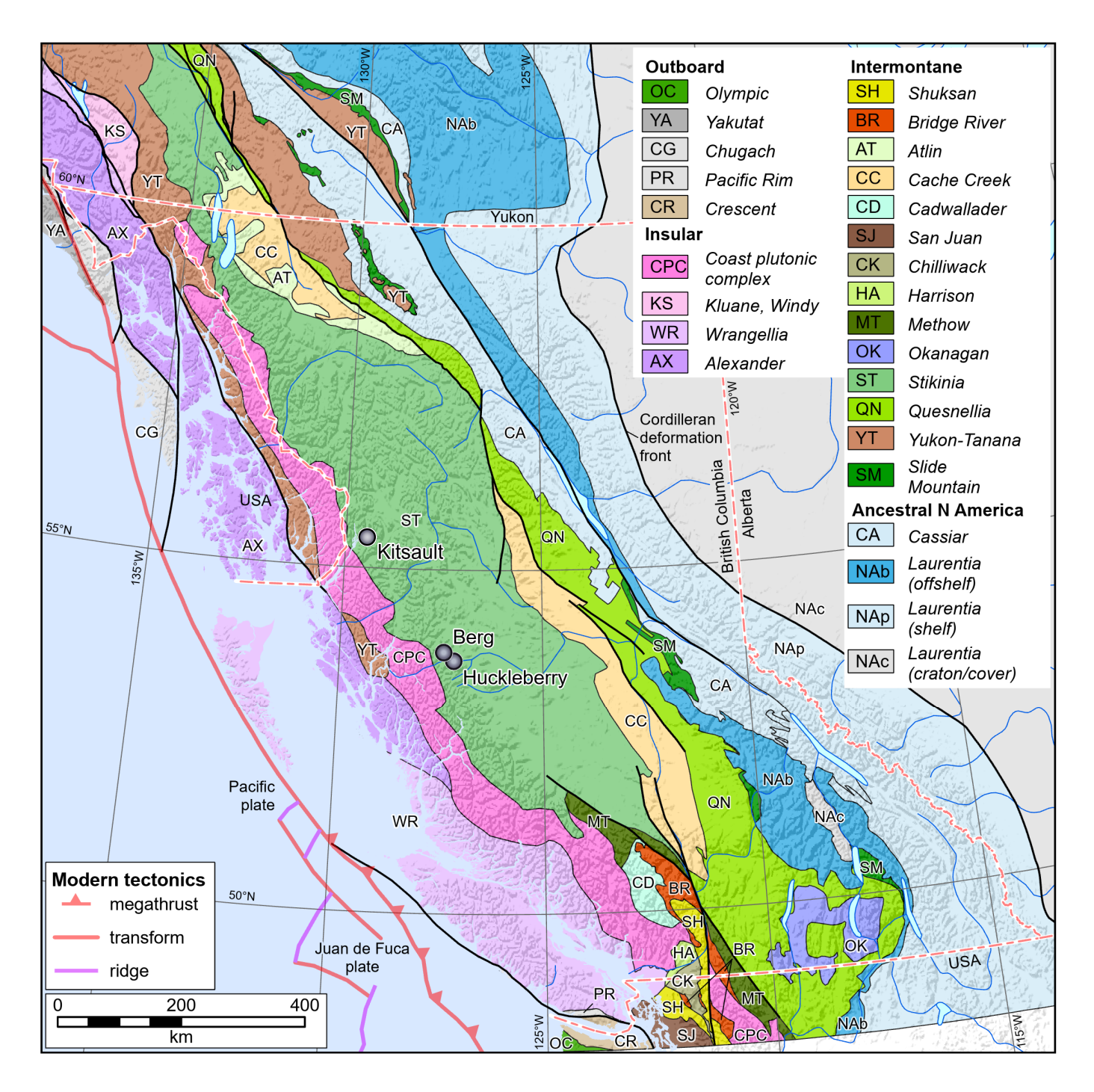


Fig. 1. Location of Kitsault, Huckleberry, and Berg deposits in Stikine terrane. Terranes modified from Colpron (2020).

(LA-ICPMS) U-Pb zircon analyses (Appendix 3); data from chemical abrasion isotope dilution thermal ionization mass spectrometry (CA-TIMS) U-Pb zircon analyses (Appendix 4); data from Re-Os molybdenite analyses (Appendix 5); concordia and weighted mean plots for igneous zircon samples (Appendix 6); cathodoluminescence (CL) images from zircon analyses (Appendix 7); S-isotope data (Appendix 8); modal mineralogy of thin sections from SEM-MLA (Appendix 9) and SEM-MLA images (Appendix 10).

2. Methods

2.1. Whole-rock geochemistry methods

2.1.1. Sample preparation

A total of 100 samples for geochemistry were collected from drill core (n=97) and outcrop (n=3) in 2023. Hand specimens and drill core samples were prepared at the British Columbia Geological Survey laboratory. Samples were cut, crushed using a steel jaw crusher, and sieved to isolate the 0.5 to 2 mm fraction. Coarse crush that did not pass through a 10 mesh (2

mm) was retained; the fine fraction that passed through 35 mesh (<500 μ m) was discarded. A chromium-steel ring and puck mill dedicated to mineralized samples was used to pulverize each sample for 20 seconds; pulps were then screened to 100% through 200 mesh (<74 μ m) using a stainless-steel sieve. The mill was cleaned between each sample by pulverizing \sim 40 g of silica sand and wiping all parts with ethanol. Coarse silica blanks were pulverized sequentially in the sample stream. Approximately 20 g of <74 μ m pulp was sent to ALS Canada Ltd., North Vancouver, for geochemical analysis. Remaining sample material, crush, and pulp were archived.

2.1.2. Analytical methods

At ALS Canada Ltd., subsamples of the pulps were analyzed by a package that varies digestion and analysis methods between analytes (method CCP-PKG01; ALS, 2024). Samples that returned greater than the detection range for specific analytes were re-analyzed with ore-grade methods while maintaining consistency in the digestion method (Appendix 1, Attributes). For analytes that yielded greater than detection ranges, results from the ore-grade methods supersede previous results.

Major-element oxides were measured by method ME-ICP06 (ALS, 2024). A 0.1 g subsample was mixed with a Li borate flux and fused in a furnace at 1025°C. The melt was cooled and dissolved in nitric, hydrochloric, and hydrofluoric acid, and the resultant solution was analyzed by inductively coupled plasma (ICP) atomic emission spectroscopy (AES). Results were corrected for inter-element spectral interference before being reported; total (%) and loss on ignition (LOI%) values were included. Trace (lithophile) elements (e.g., Ba, Ga, Ge, Sn, U, V, W) were measured by method ME-MS81 (ALS, 2024), which uses the same Li borate fusion and acid digestion as ME-ICP06 followed by ICP-mass spectrometry (MS) analysis. This fusion is considered the best method for complete dissolution of trace elements from silicates, although some zircon, metal oxides, rare-earth phosphates, and sulphides may not be fully recovered (ALS, 2024).

Base metals (Ag, Cd, Co, Cu, Li, Mo, Ni, Pb, and Zn) were analyzed with method ME-4ACD81, which uses ICP-AES following Li borate fusion and digestion of a 0.25 g subsample in a 4-acid (perchloric, nitric, hydrofluoric, hydrochloric) solution. Samples that yielded greater than the detection ranges (100 ppm Ag, 1000 ppm Cd, or 1% of Pb, Zn, and Cu) were reanalyzed for single analytes with method ME-OG62, a 4-acid digestion on 0.4 g subsample followed by ICP-AES analysis. One sample yielded >20% Pb and was re-analyzed using Pb-OG62h, a high-grade version of the same method. Two samples yielded >1500 ppm Ag and were re-analyzed by fire assay with a gravimetric finish on a 30 g sub-sample (Ag-GRA21). Five samples that yielded >1000 ppm Cd were re-analyzed using ME-ICP41a, as above.

Carbon and S were analyzed by LECO Infrared Spectroscopy (ME-IR08) in which a sample is combusted in a high-frequency LECO induction furnace in a stream of oxygen that converts S into SO₂ and C into CO₂. The resultant gas was passed directly into a cell with infrared (IR) energy, which absorbed the SO₂

and CO₂ at different wavelengths. Absorption was quantitatively detected and used to calculate total S and total C.

Volatile trace elements (e.g., As, Bi, Hg, In, Sb, Te) were analyzed (0.5 g subsample) by ICP-MS using collision cell technology for lowest detection limits following 45-minute digestion by aqua regia. The resulting solution was cooled, diluted to 12.5 mL with de-ionised water and mixed (ALS method ME-MS42). These elements were analyzed using relatively low-temperature aqua regia digestion to avoid volatilization as is common with higher temperature four-acid digestion or fusion methods. Several of these analytes yielded greater than the detection ranges (As, Bi, Hg, Sb), and were further analyzed with ME-ICP41a, an intermediate level aqua regia (ICP-AES) method with higher upper and lower detection limits.

For samples of sufficient quantity, Au and platinum group metals (Pt, Pd, Rh, Ir, Os, and Ru) were analyzed by ICM-MS following nickel sulphide collection fire assay (PGM-MS25NS). It is noted that Au may be under-reported using this method (ALS, 2024).

2.1.3. Quality assurance

A total of 10 quality control samples (silica blanks, pulp duplicates, and standards) were inserted into the sample stream at the BCGS preparatory laboratory (Appendix 1, Data).

2.1.3.1. Preparation blanks

To monitor sample preparation contamination, four coarse silica sand blanks (Sigma-Aldrich-certified as \geq 99.995 weight% SiO₂) were pulverized in the same manner as routine samples (Appendix 1, Blanks-contamination). Analytical results from silica blanks indicate Cu concentrations \leq 170 ppm (with 4 ppm Mo) and Pb and Zn concentrations typically 10-20 ppm.

2.1.3.2. Pulp duplicates

To assess precision of the results, four pulp duplicates were split from their parent sample after pulverization (Appendix 1, Duplicates-precision). The pulp duplicates represent the homogeneity of the pulp after pulverization and analytical reproducibility (precision). Analytical precision is assessed by performance of the pulp duplicates relative to their parent samples. Relative analytical precision is estimated by the average coefficient of variation, CV_{AVR} (%) for 4 data pairs (parent-duplicate) (e.g., Van der Vlugt et al., 2022).

$$CV_{AVR}$$
 (%) = 100 $\sqrt{\frac{2}{N} \sum_{i=1}^{N} \left(\frac{(a_i - b_i)^2}{(a_i + b_i)^2}\right)}$ Eqn. 1

where a_i and b_i are the analytical results for the i^{th} pair of duplicate samples, and N is the number of the data pairs (Abzalov, 2008). In cases where analytes were below the detection range for the given method, the values were replaced with ½ LoD (e.g., <5 ppm was replaced with 2.5 ppm) for the calculation of CV_{AVR} .

We consider that CV_{AVR} values of <20% indicate generally acceptable precision. Several key analytes including Ag, As, Bi, Cd, Cu, Mo, Pb, Sb, Se, Te, and Zn yielded >20% CV_{AVR} . This poor replication of duplicates may be a result of heterogeneity of the pulp, poor analytical precision, or a combination of the two factors.

2.1.3.3. Standards

Two standards were included in the sample stream as pulps (Appendix 1, Standards-accuracy). The results from these reference materials can be used to assess analytical accuracy, which is the analytical result relative to their recommended or certified values and standard deviation (or 95% confidence interval). Standards included Canadian Certified Reference Materials Project CANMET TDB-1 (n=1), and the BCGS-Till-2013 homogenized bulk sample.

For replicate analyses of standards, accurate or unbiased analytical results for each analyte satisfy the following condition:

$$\frac{|m-\mu|}{2\sqrt{\sigma_L^2 + \frac{S_w^2}{n}}} \le 1$$
 Eqn. 2

where m is the average of replicate analyses (or the result if n=1), μ is the recommended or certified reference mean (i.e., expected value/EV), σ_L is the interlaboratory certified standard deviation, n is the number of analyses (i.e., n=1 or 2), and $S_w = CV_{AVR} * m$ (representing analytical precision) (e.g., Van der Vlugt et al., 2022). The analytical results for TDB-1 are accurate for certified values of Cu, Ni, Zn, Ba, Ce, Cr, and provisional values of As, Co, Pb, Sb, Dy, Eu, Ga, Hf, Ho, La, Li, Lu, Mo, Rb, Sc, Sm, Sn, Sr, Ta, Tb, Ti, Tm, U, V, Y, Yb, and Zr. The analytical results for BCGS-Till-2013 are accurate for most analytes (including Ag, As, Bi, Cd, Co, Cu, Mo, Ni, Pb, Sb, Se, Zn) and marginally accurate for V, SiO₂, Li, and Zr. The relatively poor precision (i.e., large CV_{AVR} values), represented by S_w in Equation 2, has the effect of increasing the tolerance for accuracy.

2.2. U-Pb zircon (LA-ICP-MS) methods

Zircons were handpicked in alcohol from rock samples that underwent standard mineral separation procedures. The entire zircon separate was placed in a muffle furnace at 900°C for 60 hours in quartz beakers to anneal minor radiation damage; annealing enhances cathodoluminescence (CL) emission and promotes more reproducible interelement fractionation during laser ablation inductively coupled plasma mass spectrometry (LA-ICPMS). Following annealing, individual grains from all samples were hand-picked based on morphology, clarity, and the absence of inclusions and mounted in epoxy for imaging, along with reference materials. Grain mounts were wet ground with carbide abrasive paper and polished with diamond paste. Cathodoluminescence (CL) imaging was carried out on a Philips XL-30 scanning electron microscope (SEM) equipped with

a Bruker Quanta 200 energy-dispersion X-ray microanalysis system at the Electron Microbeam/Xray Diffraction Facility (EMXDF) at the University of British Columbia. An operating voltage of 15 kV was used, with a spot diameter of 6 μm and peak count time of 17-27 seconds. After removal of the carbon coat the grain mount surface was washed with mild soap and rinsed with high purity water. Before analysis the grain mount surface was cleaned with 3 N HNO₃ acid and again rinsed with high purity water to remove any surficial Pb contamination that could interfere with the early portions of the spot analyses.

Analyses were conducted using a Resonetics RESOlution M-50-LR, which contains a Class I laser device equipped with a UV excimer laser source (Coherent COMPex Pro 110, 193 nm, pulse width of 4 ns) and a two-volume cell designed and developed by Laurin Technic Pty. Ltd. (Australia). This sample chamber allowed investigating several grain mounts in one analytical session. The laser path was fluxed by N₂ to ensure better stability. Ablation was carried out in a cell with a volume of approximately 20 cm³ and a He gas stream that ensured better signal stability and lower U-Pb fractionation (Eggins et al., 1998). The laser cell was connected via a Teflon squid to an Agilent 7700x quadrupole ICP-MS housed at PCIGR. A pre-ablation shot was used to ensure that the spot area on grain surface was contamination-free. Samples and reference materials were analyzed for 36 isotopes: ⁷Li, ²⁹Si, ³¹P, ⁴³Ca, ⁴⁵Sc, ⁴⁹Ti, Fe (⁵⁶Fe, ⁵⁷Fe), ⁸⁹Y, ⁹¹Zr, ⁹³Nb, ⁹⁵Mo, ⁹⁸Mo, ¹³⁹La, ¹⁴⁰Ce, ¹⁴¹Pr, ¹⁴⁶Nd, ¹⁴⁷Sm, ¹⁵³Eu, ¹⁵⁷Gd, ¹⁵⁹Tb, ¹⁶³Dy, ¹⁶⁵Ho, ¹⁶⁶Er, ¹⁶⁹Tm, ¹⁷²Lu, ¹⁷⁷Hf, ¹⁸¹Ta, ²⁰²Hg, Pb (²⁰⁴Pb, ²⁰⁶Pb, ²⁰⁷Pb, ²⁰⁸Pb), ²³²Th, and U (235U, 238U) with a dwell time of 0.02 seconds for each isotope. Pb/U and Pb/Pb ratios were determined on the same spots along with trace element concentration determinations. These isotopes were selected based on their relatively high natural abundances and absence of interferences. The settings for the laser were: spot size of 34 µm with a total ablation time of 30 seconds, frequency of 5 Hz, fluence of 5 J/cm², power of 7.8 mJ after attenuation, pit depths of approximately 15 µm, He flow rate of 800 mL/min, N, flow rate of 2 mL/min, and a carrier gas (Ar) flow rate of 0.57 L/min.

Reference materials were analyzed throughout the sequence to allow for drift correction and to characterize downhole fractionation for Pb/U and Pb/Pb isotopic ratios. For trace elements, NIST 612 glass was used for both drift correction and trace element calibration, with sample spacing between every five to eight unknowns, and 90Zr was used as the internal standard assuming stoichiometric values for zircon. NIST 610 glass was analyzed after each NIST 612 analysis and used as a monitor reference material for trace elements. For U-Pb analyses, natural zircon reference materials were used, including Plešovice (Sláma et al., 2008; 337.13 ± 0.33 Ma) or 91500 (Wiedenbeck et al., 1995; 2004; 1062.4 ± 0.4 Ma, ²⁰⁶Pb/²³⁸U date) as the internal reference material, and both Temora2 (Black et al., 2004; 416.78 \pm 0.33 Ma) and Plešovice and/or 91500 as monitoring reference materials; the zircon reference materials were placed between the unknowns in a similar fashion as the NIST glasses. Raw data were reduced using the Iolite 3.4 extension (Paton et al., 2011) for Igor ProTM yielding concentration values, Pb/U and Pb/Pb dates, and their respective propagated uncertainties. For all LA-ICPMS analyses, individual grain ages with <0.05 probability of concordance were excluded (calculated using IsoplotR, Vermeesch, 2018).

2.3. U-Pb zircon (CA-TIMS) methods

Chemical abrasion isotope dilution thermal ionization mass spectrometry (CA-TIMS) procedures described here are modified from Mundil et al. (2004), Mattinson (2005), and Scoates and Friedman (2008). After zircons were analyzed by LA-ICPMS, selected zircon grains were transferred into clean 300 mL PFA microcapsules (crucibles) and ultrapure HF (up to 50% strength, 500 mL) and HNO₂ (up to 14N, 50 mL) were added for chemical abrasion leaching step. They were placed in 125 mL PTFE liners (up to 15 per liner) and about 2 mL HF and 0.2 mL 3.5N HNO₂ of the same strength as acid in beakers containing samples were added to the liners. The liners were then slid into stainless steel Parr high pressure dissolution devices, which were sealed and brought up to a maximum of 190°C for 8-16 hours (typically 175°C for 12 hours). Beakers are removed from liners and zircon is separated from leachate. Zircons were rinsed with >18 M Ω .cm water and 3.5N HNO₂. Then 200 µL of sub-boiled 6N HCl was added, and beakers were set on a hotplate at 80-130°C for 30 minutes and again rinsed with water. For full dissolution in same microcapsules (crucibles), about 50 µL 50% HF and 5 µL 14N HNO, were added, and each was spiked with a 233-235U-205Pb tracer solution (EARTHTIME ET535), capped and again placed in a Parr liner (up to 15 microcapsules per liner). Zircon was dissolved in Parr vessels in 120 µL of 29M HF with a trace of 3.5M HNO₂ at 220°C for 48 h, dried to fluorides, and re-dissolved in 6M HCl at 180°C overnight. Solutions were subsequently dried down and redissolved in 60 µL of 3M HCl to convert to PbCl₂-, UO₂Cl₂-, and UCl₄-ions. U and Pb were separated from the zircon matrix using an HCl-based anion-exchange chromatographic procedure. Pb was eluted with 200 μL of 6M HCl and U with 250 µL of MQ-H₂O into the same beaker and dried with 2 µL of 0.05 N H₂PO₄.

Pb and U were loaded on a single outgassed Re filament in 5 μL of a silica gel/phosphoric acid mixture (Gerstenberger and Haase, 1997), and U and Pb isotopic measurements were made on a Nu Instruments thermal ionisation mass spectrometer equipped with an ion-counting Daly detector. Pb isotopes were measured in static mode for all isotopes on 150 cycles on 10 second intervals on $10^{13}\Omega$ resistors for masses 208-205 with mass 204 measured on the Daly detector. Mass fractionation was determined using repeat measurements of standard material NBS-981 solution that has equal atom ²⁰⁸Pb and ²⁰⁶Pb and thus measures fractionation directly and was $0.16\pm0.03\,\%\,\mathrm{amu^{-1}}$ for the analytical sessions reported here. Transitory isobaric interferences due to high-molecularweight organics, particularly on 204Pb and 207Pb, disappeared within approximately 20 cycles, while ionization efficiency averaged 10 mVpg⁻¹ of each Pb isotope. Linearity (to cps) and the associated deadtime correction of the Daly detector were monitored by repeated analyses of NBS981. Uranium was analyzed as UO ions in static Faraday mode on 10¹³ Ω resistors for 200 cycles and corrected for isobaric interference of ²³³U¹⁸O¹⁶O on ²³⁵U¹⁶O¹⁶O with an ¹⁸O/¹⁶O ratio of 0.00206. Ionization efficiency averaged 20 mVng⁻¹ of each U isotope. U mass fractionation was corrected using the known ²³³U/²³⁵U ratio of the tracer solution.

U-Pb dates and uncertainties were calculated using the algorithms of Schmitz and Schoene (2007); calibration of ET535 tracer solution (Condon et al., 2015) of $^{235}\text{U}/^{205}\text{Pb}$ = 100.233, $^{233}\text{U}/^{205}\text{Pb}$ = 0.99506, and $^{205}\text{Pb}/^{204}\text{Pb}$ = 11268; U decay constants recommended by Jaffey et al. (1971); and of $^{238}\text{U}/^{235}\text{U}$ = 137.818 (Hiess et al., 2012). The $^{206}\text{Pb}/^{238}\text{U}$ ratios and dates were corrected for initial ^{230}Th disequilibrium using δ Th/U = 0.20±0.05 (1 σ) and the algorithms of Crowley et al. (2007), resulting in an increase in the $^{206}\text{Pb}/^{238}\text{U}$ dates of \sim 0.09 Ma. All common Pb in analyses was attributed to laboratory blank and subtracted based on the measured laboratory Pb isotopic composition and associated uncertainty. Uranium blanks are estimated at 0.013 pg.

Weighted mean ²⁰⁶Pb/²³⁸U dates are calculated from equivalent dates (probability of fit >0.05) using Isoplot 3.0 (Ludwig, 2003). Errors on the weighted mean dates are given as X (Y) [Z]. X is the internal error based on analytical uncertainties only, including counting statistics, subtraction of tracer solution, and blank and initial common Pb subtraction, and Y errors include the uncertainty in the tracer calibration propagated in quadrature. Internal errors should be considered when comparing these CA-TIMS dates with those derived from other geochronological methods using the U-Pb decay scheme (e.g., LA-ICPMS). Z errors include uncertainties in the tracer calibration and ²³⁸U decay constant (Jaffey et al., 1971) and should be considered when comparing our dates with those derived from other decay schemes (e.g., ⁴⁰Ar/³⁹Ar, ¹⁸⁷Re-¹⁸⁷Os).4***

2.4. Re-Os methods

Methods used for molybdenite Re-Os analysis are described in detail by Selby and Creaser (2004). Areas of each sample with visible molybdenite were selected, and preparation of a molybdenite mineral separate was made by metal-free crushing and sieving followed by magnetic and gravity concentration methods. The ¹⁸⁷Re and ¹⁸⁷Os concentrations in molybdenite were determined by isotope dilution mass spectrometry using Carius-tube, solvent extraction, anion chromatography and negative thermal ionization mass spectrometry techniques. For this work, a mixed, double-Os spike containing known amounts of isotopically enriched ¹⁸⁵Re, ¹⁹⁰Os, and ¹⁸⁸Os analysis was used (Markey et al., 2007). Isotopic analysis used a ThermoScientific Triton mass spectrometer by Faraday collector. Total procedural blanks for Re and Os are less than <3 picograms and <0.5 picograms, respectively, which are insignificant in comparison to the Re and Os concentrations in molybdenite. The Reference Material 8599 Henderson molybdenite (Markey et al., 2007) is routinely analyzed as a standard, and during the past 2 years returned an average Re-Os date of 27.83 ± 0.09 Ma (n=14), indistinguishable within uncertainty from the Reference Age Value of 27.66 ± 0.1 Ma (Wise and Watters, 2011). The ¹⁸⁷Re decay constant used is $1.666 \times 10^{-11} \, \mathrm{a}^{-1}$ (Smoliar et al, 1996).

2.5. S-isotope methods

At the BCGS preparation laboratory, a hand-held drill was used to extract 124 pulp samples into glass vials from coarse grains of pyrite, chalcopyrite, sphalerite, galena, magnetite, tetrahedrite, molybdenite, and anhydrite. These were sent to Queen's Facility for Isotope Research (QFIR) for analysis of sulfur (S) isotopes. At QFIR, samples were weighed into tin capsules and the sulfur isotopic compositions were measured using a MAT 253 Stable Isotope Ratio Mass Spectrometer coupled to a Costech ECS 4010 Elemental Analyzer.

Values of $\delta^{34}S$ were calculated by calibrating results to certified reference materials and then normalizing the $^{34}S/^{32}S$ ratios in the sample to that in the Vienna Canyon Diablo Troilite (VCDT) international standard. Values are reported using the delta (δ) notation in units of permille (δ) and are reproducible to 0.2%. An additional 10% of QA/QC samples included three standards and two duplicate analyses, which were used to calculate precision of 0.2%. Accuracy is based upon primary or secondary standard analyses as follows: isotope $\delta^{34}S$ standard deviation 0.3%.

2.6. Petrography and scanning electron microscopy methods

Polished thin sections were examined using a scanning electron microscope (SEM) and derived backscatter electron (BSE) images, and quantitative mineral abundance maps and determinations by mineral liberation analysis (MLA). The SEM work was undertaken at the CREAIT Microanalysis Facility (MAF), Memorial University, using a FEI MLA 650 field emission gun SEM equipped with two Brucker silicon drift EDS detectors. Operating conditions included 25 kV accelerating voltage for BSE images. Operating conditions for MLA included a 25 kV accelerating voltage, 10 nA current, and a 5.85 electron beam spot size. Thin sections were measured in GXMAP (grain-based X-ray mapping) mode where X-ray analyses were triggered for a BSE range of 40 to 255. Each X-ray measurement was acquired for 12 ms on a 1.5 by 1.5 mm frame with a resolution of 500 pixels per frame and an imaging scan speed of 16 µsec. Data reduction was performed on MLA Data View (FEI) software version 3.1.4.683.

References cited

Abzalov, M., 2008. Quality control of assay data: A review of procedures for measuring and monitoring precision and accuracy. Exploration and Mining Geology, 17, 131-144.

https://doi.org/10.2113/gsemg.17.3-4.131
ALS, 2024. Geochemistry schedule of services and fees CAD 2024.
Last accessed November 28, 2024.

https://www.alsglobal.com/en/geochemistry/geochemistry-feeschedules

Black, L.P., Kamo, S.L., Allen, C.M., Davis, D.W., Aleinikoff, J.N., Valley, J.W., Mundil, R., Campbell, I.H., Korsch, R.J, Williams, I.S., and Foudoulis, C., 2004. Improved ²⁰⁶Pb/²³⁸U microprobe geochronology by the monitoring of a trace-element-related matrix effect; SHRIMP, ID–TIMS, ELA–ICP–MS and oxygen isotope documentation for a series of zircon standards. Chemical Geology, 205, 115-140.

Colpron, M., 2020. Yukon Terranes-A digital atlas of terranes for the northern Cordillera. Yukon Geological Survey. data.geology.gov.yk.ca/Compilation/2#InfoTab

Condon, D.J., Schoene, B., McLean, N.M., Bowring, S.A., and Parrish, R.R., 2015. Metrology and traceability of U–Pb isotope dilution geochronology (EARTHTIME Tracer Calibration Part I). Geochimica et Cosmochimica Acta., 164, 464-480. https://doi.org/10.1016/j.gca.2015.05.026

Crowley, J.L., Schoene, B., and Bowring, S.A., 2007. U-Pb dating of zircon in the Bishop Tuff at the millennial scale. Geology, 35, 1123–1126.

https://doi.org/10.1130/G24017A.1

Eggins, S.M., Kinsley, L., and Shelley, J., 1998. Deposition and element fractionation processes during atmospheric pressure laser sampling for analysis by ICP-MS. Applied Surface Science, 127-129, 278-286.

https://doi.org/10.1016/S0169-4332(97)00643-0

Gerstenberger, H., and Haase, G., 1997. A Highly effective emitter substance for mass spectrometric Pb isotopic ratio determinations. Chemical Geology, 136, 309-312.

Hickin, A.S., Ootes, L., Orovan, E.A., Brzozowski, M.J., Northcote, B.K., Rukhlov, A.S., and Bain, W.M., 2024. Critical minerals and mineral systems in British Columbia. In: Geological Fieldwork 2023, British Columbia Ministry of Energy, Mines and Low Carbon Innovation, British Columbia Geological Survey Paper 2024-01, pp. 13-51.

Hiess, J., Condon, D.J., McLean, N, and Noble S.R., 2012. ²³⁸U/²³⁵U Systematics in terrestrial uranium-bearing minerals. Science, 335, 1610-1614.

https://www.science.org/doi/10.1126/science.1215507

IGF (Intergovernmental Forum on Mining, Minerals, Metals, and Sustainable Development), 2023. Searching for critical minerals? How metals are produced and associated together, 30p. https://www.igfmining.org/resource/searching-for-critical-minerals-how-metals-are-produced-and-associated-together/

Jaffey, A.H., Flynn, K.F., Glendenin, L.E., Bentley, W.C., and Essling, A.M., 1971. Precision measurement of half-lives and specific activities of ²³⁵U and ²³⁸U. Physical Review C, 4, 1889-

John, D.A., and Taylor, R.D., 2016. By-products of porphyry copper and molybdenum deposits. Reviews in Economic Geology, 18, 137-164.

Lawley, C.J.M., Petts, C.C., Lee, W., Cajal, Yl., Carrasco-Godoy, C., Campbell, I.H., Dlugosz, J., Larson, K.P., Savard, D., Kjarsgaard, I, and van Stratten, B.I., 2025. Critical raw material potential of porphyry copper-gold deposits in the Golden Triangle, northwest British Columbia, Canada. Ore Geology Reviews, 178, article 106463.

https://doi.org/10.1016/j.oregeorev.2025.106463

Ludwig, K.R., 2003. Isoplot 3.00: A geochronological toolkit for Microsoft Excel. Special Publication, Berkley Geochronology Center, 70p.

Markey, R., Stein, H.J., Hannah, J.L., Selby, D., and Creaser, R.A., 2007. Standardizing Re-Os geochronology: A new molybdenite

- reference material (Henderson, USA) and the stoichiometry of Os salts. Chemical Geology, 244, 74-87.
- Mattinson, J.M., 2005. Zircon U-Pb chemical abrasion ("CA-TIMS") method: Combined annealing and multi-step partial dissolution analysis for improved precision and accuracy of zircon ages. Chemical Geology, 220, 47–66.
- Miller, E.A., Ferri, M.D., Wall, C., Creaser, R.A., van Straaten, B.I., and Graham, A.C., 2025. New geochronologic data, Kitsault River area, northwestern British Columbia: Igneous zircons (high-precision CA-TIMS), detrital zircons (LA-ICP-MS), and molybdenite (Re-Os). British Columbia Ministry of Mining and Critical Minerals, British Columbia Geological Survey GeoFile 2025-21, 6 p.
- Mudd, G.M., Yellishetty, M., Reck, B.K., and Graedel, T.E., 2014. Quantifying the recoverable resources of companion metals: A preliminary study of Australian mineral resources. Resources, 3, 657-671.

https://doi.org/10.3390/resources3040657

- Mudd, G.M., Jowitt, S.M., and Werner, T.T., 2017. The world's byproduct and critical metal resources part I: Uncertainties, current reporting practices, implications and grounds for optimism. Ore Geology Reviews, 86, 924-938.
- Mundil, R., Ludwig, K. R., Metcalfe, I., and Renne, P. R., 2004. Age and timing of the Permian mass extinctions: U/Pb dating of closed-system zircons. Science, 305, 1760-1763.
- Nassar, N.T., Graedel T.E., and Harper, E.M., 2015. By-product metals are technologically essential but have problematic supply. Science Advances, article 1400180.

https://doi.org/10.1126/sciadv.1400180

- NRCan (Natural Resources Canada), 2024. Critical Minerals List. Government of Canada.
 - https://www.canada.ca/en/campaign/critical-minerals-in-canada/critical-minerals-an-opportunity-for-canada.html (last accessed December 27, 2024)
- Orovan, E.A., Zaborniak, K., and Hooker, K., 2024. Textural evidence for ore fluid transport and the magmatic to hydrothermal transition at the past-producing Kitsault Mo-Ag mine. In: Geological Fieldwork 2023, British Columbia Ministry of Energy, Mines and Low Carbon Innovation, British Columbia Geological Survey Paper 2024-01, pp. 53-64.
- Orovan, E.A., Ebert, S., Baldazzi, P., Saxton, D., and Goudie, D.J., 2025. Critical minerals at the Berg and Huckleberry porphyry deposits, British Columbia, using scanning electron microscropymineral liberation analysis (SEM-MLA). In: Geological Fieldwork 2024, British Columbia Ministry of Mining and Critical Minerals, British Columbia Geological Survey Paper 2025-01, pp. 73-84.
- Paton, C., Hellstrom, J., Paul, B., Woodhead, J., and Hergt, J., 2011. Iolite: Freeware for the visualization and processing of mass spectrometric data. Journal of Analytical Atomic Spectometry, 26, 2508-2518.
- Scoates, J. S., and Friedman, R. M., 2008. Precise age of the platiniferous Merensky Reef, Bushveld Complex, South Africa, by the U-Pb ID-TIMS chemical abrasion ID-TIMS technique. Economic Geology, 103, 465-471.
- Schmitz, M. D., and Schoene, B., 2007. Derivation of isotope ratios, errors, and error correlations for U-Pb geochronology using ²⁰⁵Pb-²³⁵U-(²³³U)-spiked isotope dilution thermal ionization mass spectrometric data. Geochemistry, Geophysics, Geosystems, 8, 20. https://doi.org/10.1029/2006GC001492
- Selby, D., and Creaser, R.A., 2004. Macroscale NTIMS and microscale LA-MC-ICP-MS Re-Os isotopic analysis of

- molybdenite: Testing spatial restrictions for reliable Re-Os age determinations, and implications for the decoupling of Re and Os within molybdenite. Geochimica et Cosmochimica Acta, 68, 3897-3908.
- Sláma, J., Košler, J., Condon, D., and Crowley, J., 2008. Plešovice zircon A new natural reference material for U–Pb and Hf isotopic microanalysis. Chemical Geology, 249, 1-35.
- Smoliar, M., Walker, R., and Morgan, J., 1996. Re-Os ages of group IIA, IIIA, IVA, IVB iron meteorites, Science, 271, 1099-1102.
- Van der Vlugt, J., Rukhlov, A.S., and van Straaten, B.I., 2022. Lithogeochemical re-analysis of British Columbia Geological Survey archived rock samples from northwestern British Columbia. British Columbia Ministry of Energy, Mines and Low Carbon Innovation, British Columbia Geological Survey GeoFile 2022-14, 15p.
- Vermeesch, P., 2018. IsoplotR: a free and open toolbox for geochronology. Geoscience Frontiers, 9, 1479-1493.
- Wiedenbeck, M., Alle, P., Corfu, F., Griffin, W.L., Meier, M., Oberli, F., Quadt, A.V., Roddick, J.C., and Spiegel, W., 1995. Three natural zircon standards for U-Th-Pb, Lu-Hf, trace element and REE analyses. Geostandards Newsletter, 19, 1-23.
- Wiedenbeck, M., Hanchar, J.M., Peck, W.H., Sylvester, P., Valley, J., Whitehouse, M., Kronz, A., Morishita, Y., Nasdala, L., Fiebig, F., Franchi, I., Girard, J.P., Greenwood, R.C., Hinton, R., Kita, N., Mason, P.R.D., Norman, M., Ogasawara, M., Piccoli, P.M., Rhede, D., Satoh, H., Schulz-Dobrick, B., Skår, Ø., Spicuzza, M.J., Terada, K., Tindle, K., Togashi, S., Vennemann, T., Xie, Q., and Zheng, Y.F., 2004. Further characterization of the 91500 zircon crystal. Geostandards and Geoanalytical Research, 28, 9-39.
- Wise, S.A., and Watters, R.L., 2011. Reference Material 8599 Henderson Molybdenite. National Institute of Standards and Technology Report of Investigation, 30 March 2011.

